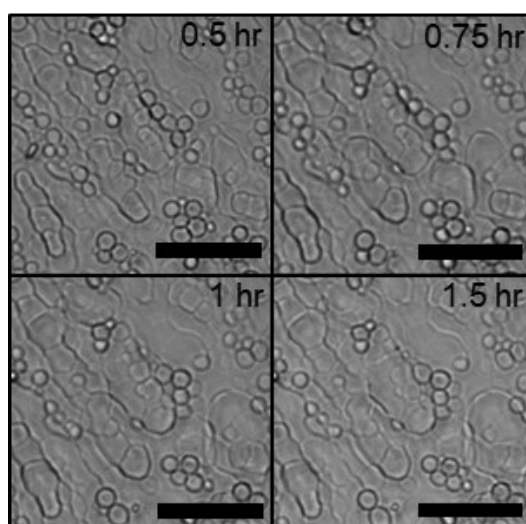


## Biologically-Active Unilamellar Vesicles from Red Blood Cells

Hyun-Sook Jang,<sup>1</sup> Yoon-Kyoung Cho,<sup>1,2</sup> and Steve Granick<sup>1,3</sup>

<sup>1</sup>Center for Soft and Living Matter, Institute for Basic Science (IBS), Ulsan 44919, South  
Korea

<sup>2</sup>Departments of Biomedical Engineering and <sup>3</sup>Chemistry, Ulsan National Institute of Science  
and Technology (UNIST), Ulsan 44919, South Korea



**Figure S1.** Bright field images of the rehydrated GUVs composed of lipids and RBC membrane in the hydrogel. Representative images at elapsed times from 0.5 to 1.5 hr show that GUV size did not change during this time; growth had saturated. The irregular background comes from accumulated differences in refractive index along the rough surface of 3-dimensional structures in agarose gel. Scale bars are 10 μm.

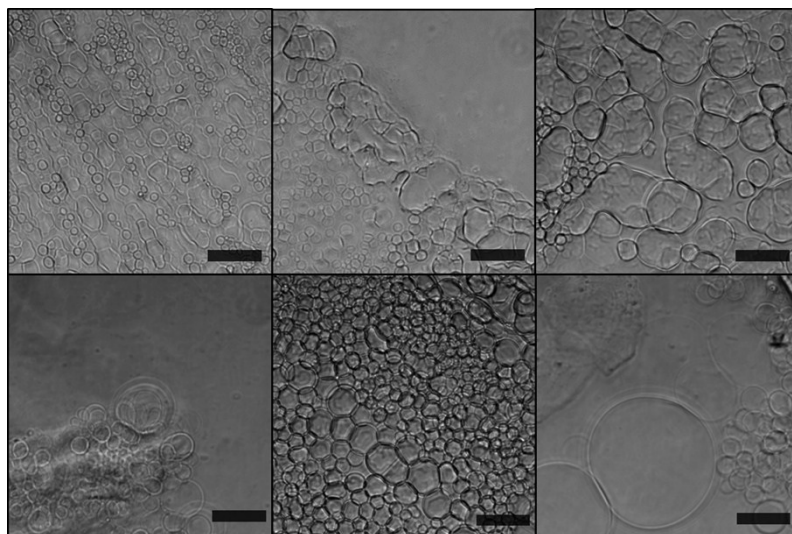


**Figure S2.** Distributions of GUVs in the final state in the agarose gel varied from spot to spot, as well as according to depth in the agarose gel. These bright field microscopy images illustrate dilute concentration in some locations, dense packing in other locations, and also vesicles fused to the agarose gel (bottom left) and occasionally a huge GUVs (bottom right). Scale bars are 10  $\mu\text{m}$ .

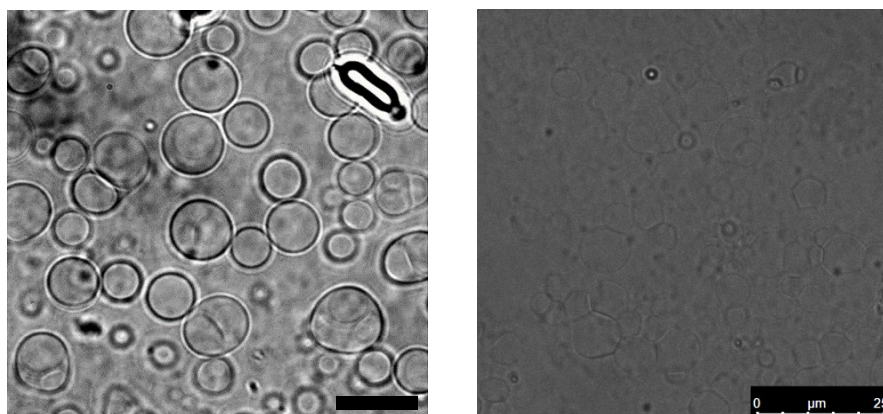


**Figure S3.** GUVs in the final state in the aqueous solution above agarose gel. The bright field microscopy images illustrate floating GUVs in x1 PBS media. Scale bar is 10 (left panel) and 25  $\mu\text{m}$  (right panel).

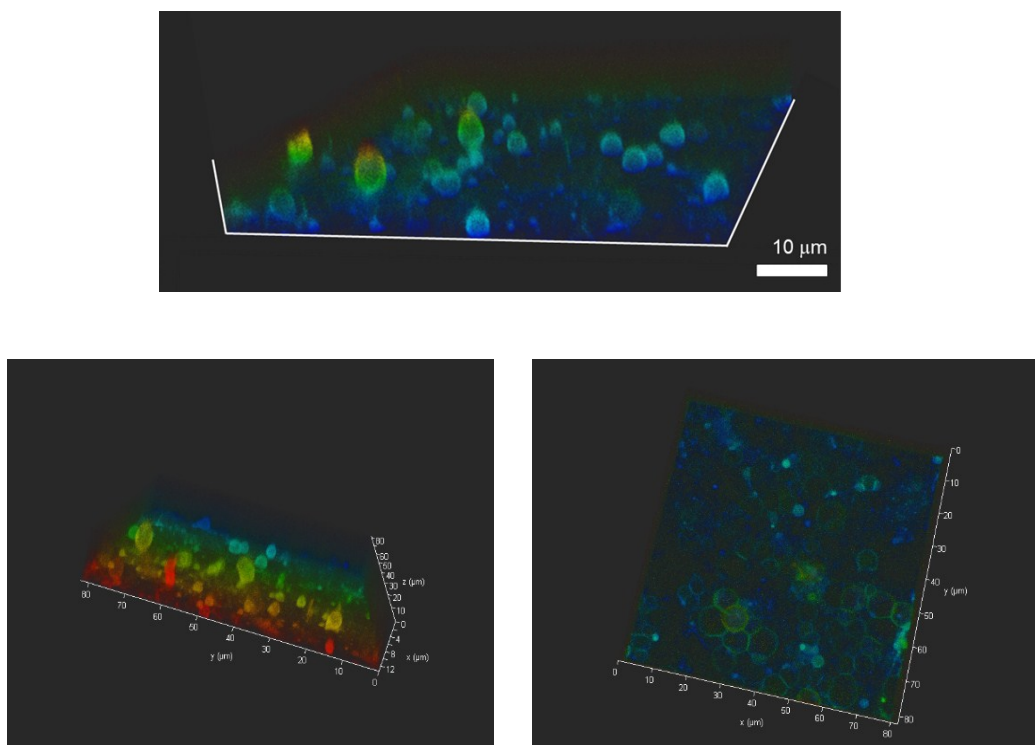


**Figure S4.** Examples of 3D reconstructed confocal images of the hybrid GUUVs while still in the agarose gel environment, illustrating their dense packing.

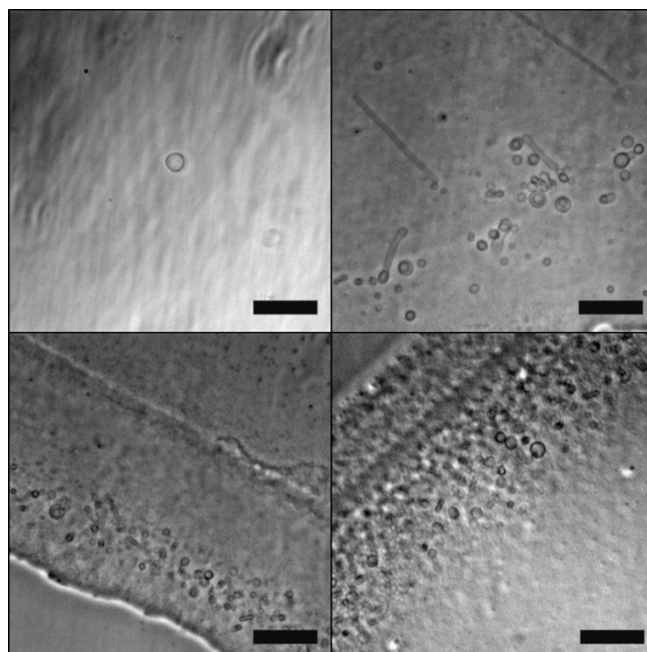


**Figure S5.** Bright field images of the RBC-membranes GUVs prepared by the combined protocol of electroformation (10V, 10Hz) and spontaneous swelling starting from small RBC-derived vesicles. The preparation began with 20-min sonication of 1 v/v % of RBC extracts to give small unilamellar vesicles (SUVs) whose size ranged from 50 to 100 nm as inferred by dynamic light scattering. These 4 illustrative images show that GUVs failed to grow above a few  $\mu\text{m}$  diameter after a few hours under physiological buffer conditions, x1 PBS. Scale bars are 10  $\mu\text{m}$ .

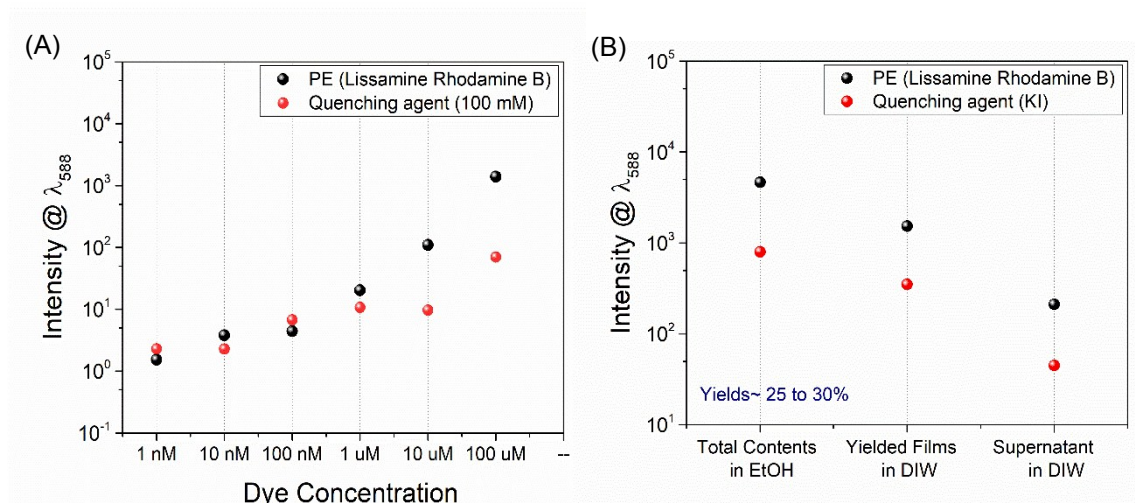


**Figure S6.** Raw data from which to estimate lipid incorporated into RBC-derived GUVs. (A) Fluorescence intensity plotted as a function of DMPE-RhBs concentration without quenching agent (black symbols) and with KI (100 mM) quenching solution (red symbols). (B) Fluorescence emitted intensity at 588 nm of the mixture used to grow GUVs: in ethanol, in deionized water (DIW), and also the supernatant in deionized water.

**Estimate of lipid incorporated into hybrid GUVs.** Figure S5(A) shows DMPE-RhB fluorescence emission as a function of dye concentration. However, the hybrid films composed of agarose, RBC membrane, and lipid possessed different solubility in water. The films and the GUV supernatant were dissolved in EtOH and deionized water (DIW), respectively, to remove the agarose. Figure S5(B) shows the fluorescence intensity at 588 nm of the total contents in EtOH, total contents in DIW, and the supernatant in DIW. The fraction of lipid incorporated into GUVs was estimated to be 25~ 30% by taking a fluorescence intensity ratio to the total contents in EtOH and DIW.

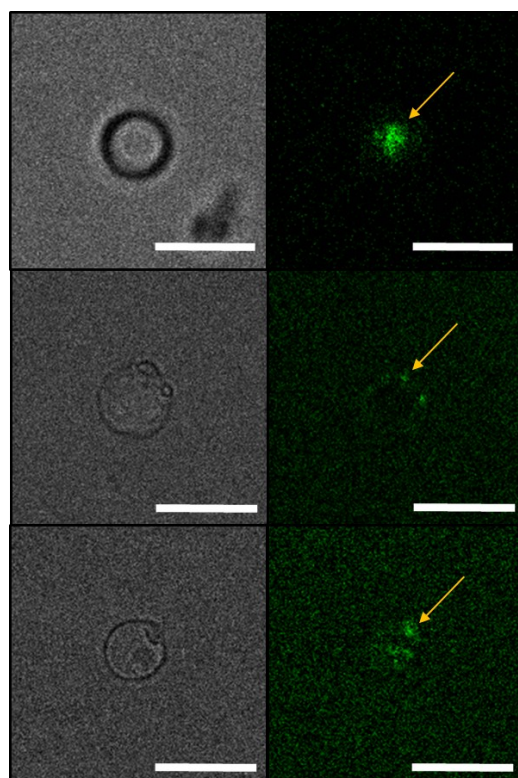


**Figure S7.** Two split images, bright field (left) and confocal microscopy (right), of the system shown in Figure 2C, further confirming inhomogeneous distribution of GLUT1 antibody along the GUV surface. Scale bars are 10  $\mu\text{m}$ . Arrows highlight the location of Alexa-488 labeled GLUT1 antibody, confirming the colocalization of GLUT1 in the GUVs.



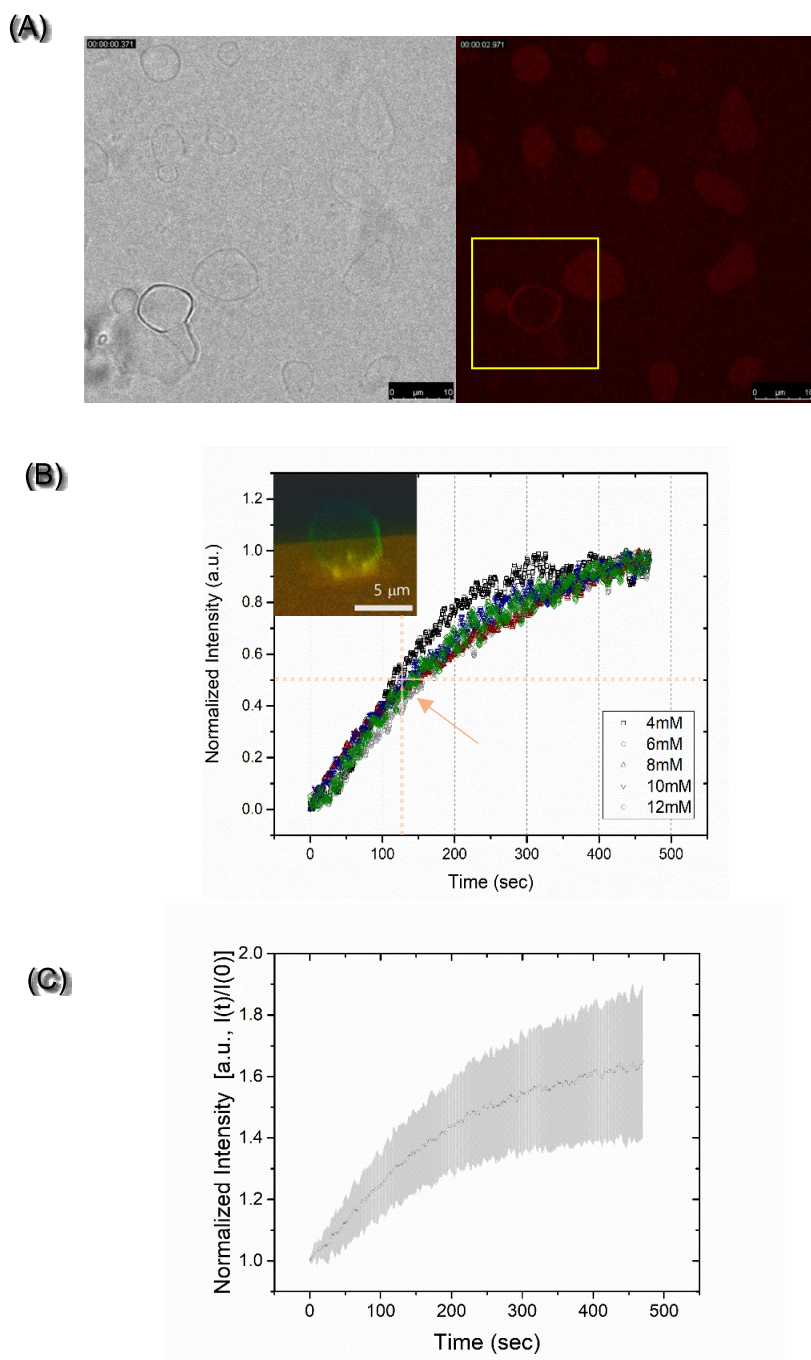


**Figure S8.** Checking for the biological activity of GLUT1, showing that different methods of analysis yield the same qualitative kinetics. (A) Bright field (left) and confocal images (right) of GUVs in hydrogel after rehydration together with the enzymes HRP, GOx, Amplex Red and buffers. (B) Time-dependent increase of fluorescence intensity in the interior, normalized to begin at zero as explained below, after adding glucose concentrations from 4 to 12 mM to the exterior solution. Color code of glucose concentration for the data points is shown in the Inset. The fluorescence intensity is normalized

by  $I = \frac{I(t) - I_{\min}(t)}{I_{\max}(t) - I_{\min}(t)}$  for comparison of kinetics under situations of different background fluorescence intensity; cf. Raza et al., *BioData Mining* 2016, 9, 11. Inset figure shows the 3D reconstructed confocal image of the surfaced-attached GUVs. (C) For the same data as in panel B, time-dependent fluorescence intensity in the interior of the surface-attached GUVs, normalized to the value at zero time, after glucose addition from 4 to 12 mM to the exterior solution. The actual fluorescence intensity increased by a factor up to  $1.65 \pm 0.25$ . The dotted line is the average. Shaded region shows span of the data under the different conditions.